Electronic Supplementary Material (ESI) for Journal of Materials Chemistry A.

Electronic Supplementary Information

Inexpensive Electrochemical Synthesis of Nickel Iron Sulfides on Nickel Foam: Super Active and Ultra-durable Electrocatalysts for Alkaline Electrolyte Membrane Water Electrolysis

Pandian Ganesan, Arumugam Sivanantham and Sangaraju Shanmugam*

Department of Energy Systems Engineering,

Daegu Gyeongbuk Institute of Science & Technology (DGIST),

50-1 Sang-Ri, Hyeongpung-Myeon, Dalseong-gun, Daegu, 42988,

Republic of Korea.

E-mail: sangarajus@dgist.ac.kr

1. Turn Over Frequency (TOF) calculation

The TOF value is calculated from the Equation 1

$$TOF = \frac{J \times A}{4 \times F \times m} \quad (1)$$

J is the current density at overpotential of 1.55 V for OER and -0.180 V for HER in A cm^{-2}. A is the area of the Ni foam electrode. F is the faraday constant (a value of 96485 C/mol). m is the number of moles of the active materials that are deposited onto the Ni foam electrode.

2. Calculation of hydrogen generation

Based on the displaced amount of water due to the hydrogen bubbles (Fig. 8a), the amount of hydrogen generated was calculated using the below relationships (2, 3).

Amount of hydrogen generated in 1 h = amount of water displaced in litres (2)

Amount of hydrogen generated in moles for 1 h = $\frac{\text{Amount of water displaced (liters)}}{22.4 \text{ liters}}$ (3)

We also calculated the hydrogen generation rate from the electrical charge passed through the electrode using the equation given below.

Current obtained During water electrolysis X Time duration for each potential = Coulomb (4)

$$\frac{\text{Coulomb} \times F}{96485C} = \text{No. of moles of } e^- \text{ for } H_2 \text{ generation} \quad (5)$$

$$\left.\frac{\text{No. of moles of electron for } H_2 \text{ generation x 1 mole of } H_2 \text{ gas}}{\text{2 mole of electron}}\right\} = \text{Moles of Hydrogen generated} \quad (6)$$

3. XPS discussion of NiFe-1/NF

The XPS spectra in Fig. S11(a) reveal signals for elemental nickel at 853.6 eV which is deviate from the 852.6 eV due to the incorporation of iron[1] and surface-adsorbed β-$Ni(OH)_2$ at 855.4 eV[2], with satellite peak at 860.8 eV. The XPS spectra in Fig. S11(b) reveal signals for elemental iron at 705.9 eV and surface-adsorbed FeOOH at 712.56 eV.[3] The presence of the nickel and iron in the elemental state confirms the existence of nickel and iron as alloy and based on the XPS peak area Fe2p and Ni2p regions, the ratio of nickel to iron calculated to be 2:1. The increased ratio of nickel may be due to the substrate. This calculated ratio is almost similarity with the XRD phase ratio of NiFe-1/NF (1:1 ratio) .

4. XPS discussion after durability Tests

After performing the OER durability test for 200 h, we used XPS to analyze the NiFeS-1/NF electrode. The XPS spectra in Fig. S8(a) reveal signals for surface-adsorbed $Ni(OH)_2$ and NiO at 858.3 and 856.2 eV, with a characteristic Ni–S signal at 861.5 eV. Unlike the Ni–S signal at 861.8 eV (Fig. 2(a)) in the fresh sample, after the OER durability test we observed the Ni-S signal at 861.5 eV (Fig. S8(a)), a shift of approximately 0.3 eV, presumably due to the detaching of nickel sulfide from NiFeS during prolonged OER operation. The formation of a new peak at 862.8 eV, along with a signal at 856.2 eV, confirmed the bonding of NiO with the nickel surface.[4-9] In Fig. S8(c), we observe the presence of $Fe_{1-x}O$ with signals at 708.6 eV in the Fe $2P_{3/2}$ region with its

satellite at 715.6 eV and a shake up signal at 723.4 eV in the Fe $2P_{1/2}$ region. After the OER durability test, the signal at 710.9 eV with its satellite peak at 714.1 eV implied the formation of FeO_2 species. In addition, Fe(II)OOH peaks appeared at 717.4 and 721.3 eV, a $FeSO_4$ peak appeared at 732.2 eV, and a Fe_2O_3 peak appeared at 737.7 eV in the Fe $2P_{1/2}$ region after the OER durability test.[9] Moreover, after the OER durability test, the spectrum of the electrode displayed (Fig. S8(e)) signals at 162.5, 163.8, 165.5, 168.7, 169.9, and 171.5 eV[5,10] related to sulfur oxidation states of NiS_2, $S^{2-}{}_n$, organic sulfur, SO_4, NiFeS, and SO_3 species, respectively.[7, 9, 11]

After the 200-h HER durability test, we also examined NiFeS-1/NF using XPS. In Fig. S8(b), a similar trend of surface-adsorbed NiO and $Ni(OH)_2$ was evident at 856.2 and 857.4 eV. Here, the nickel oxidation state relevant to Ni–S appeared again as a characteristic peak at 861.5 eV (Fig. 2(a)),[4-9] suggesting the presence of nickel sulfide with a shift of 0.4 eV from that of the fresh NiFeS-1/NF (Fig. S8(b)). Moreover, the presence of NiO bonded with the nickel surface, represented by a signal at 863.8 eV (Fig. 2(b)), supported the appreciable formation of nickel oxide during the prolonged HER operation.[5,9] In the Fe 2p spectrum in Fig. S8(d), recorded after HER of the NiFeS-1/NF catalyst, the presence of Fe_2O_3 was confirmed by the peak at 709.4 eV, with its satellite at 714.8 eV. In addition, the signal at 719.3 eV suggests the presence of Fe_2O_2, while and presence of Fe_2O_3 was confirmed by the signal at 737.4 eV. Moreover, after the HER durability test, the electrode (Fig. S8(f)) presented only three peaks at 162.5, 168.9 and 169.9 eV[5,10] relates to sulfur oxidation states for NiS_2, $FeSO_4$, and NiFeS species, respectively.[7,9-11]

For all of the tested catalysts, we observed signals for iron metal [Fe(0)] at 706.0, 707.7, and 705.7 eV before and after the OER and HER durability tests, respectively, of NiFeS-1/NF (Fig. 2(b) and

Fig. S8(c, d)).[8] The positive shift of the signal of iron in the zero oxidation state from 706 to 707.7 eV after the OER durability test of NiFeS-1/NF was due to the formation of iron oxides.

Even though, already the XPS after OER and HER of NiFeS-1/NF were discussed in supplementary information. The XPS comparison of NiFeS-1/NF among fresh, after 200 h of OER and HER stability were discussed in detail (Fig. S12.)

In the Ni2P XPS spectra, the characteristic peak of nickel iron sulphide at 861.5 eV (Fig. 2a) was observed in fresh NiFeS-1/NF, but the after OER and HER electrodes also exhibits 851.5 eV(Fig.12 a,b), respectively. This confirms the existence of the nickel iron sulphide peak even after stability tests.

In the Fe $2p_{3/2}$ spectra in Fig. 2(b) and Fig. S12 (c, d), recorded before and after the OER and HER tests, we observed signals for iron in oxidation states relevant to nickel iron sulfide composites at 725.2, 725.5, and 724.5 eV, respectively.[6,8,10] The shift in the signal for the oxidation state of iron related to the nickel iron sulfide composite after the HER test of approximately 0.7 eV from 725.2 eV may have been due to the reduction of iron atoms during the HER in the water splitting process.

In the case of S2p XPS, the presence of nickel iron sulfide characteristic peaks around 169.8 eV in fresh (Fig. 2c), after HER and OER NiFeS-1/NF (Fig. 12 e,f) electrodes. But in all the case, the characteristic peak of metal di sulfides at 162.5 eV were observed. This confirms the evidence of the presence of metal sulfide and formation of metal hydroxide is not possible. [5,8,10]

Based on the XRD after cyclic measurement and XPS after Chrono-potentiometric studies of NiFeS-1/NF, we conclude that formation of Nickel oxide and iron oxide along with the existence of nickel iron sulphide. Anyhow, presence of oxyhydroxide on nickel iron sulfides may be involved in the catalytic process.

5. XRD pattern of heat treated NiFe-1/NF, NiFeS-1/NF and Ni & S deposition on stainless steel

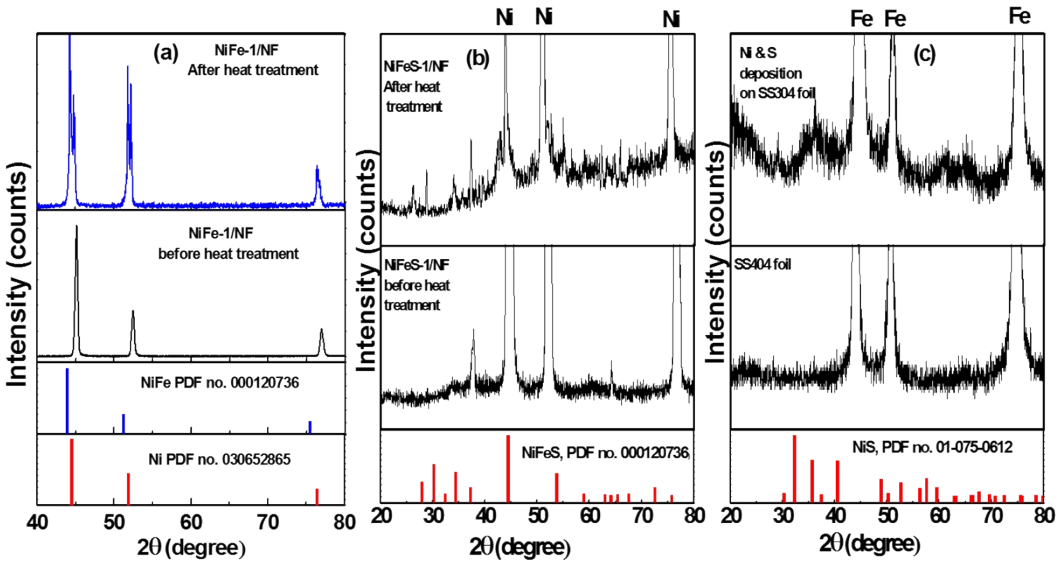

Fig. S1 (a) XRD pattern of NiFe-1/NF before and after 500 ^{0}C heat treatment. (b) XRD patterns of NiFeS-1/NF before and after heat treatment at 500 ^{0}C in Ar atmosphere. (c) XRD patterns of stainless steel (SS404 foil) and cyclic voltammetric deposition of nickel and sulfur on stainless steel (SS404)NiFeS-1/NF before and after heat treatment at 500 ^{0}C in Ar atmosphere.

6. Electrodes for water electrolyzer

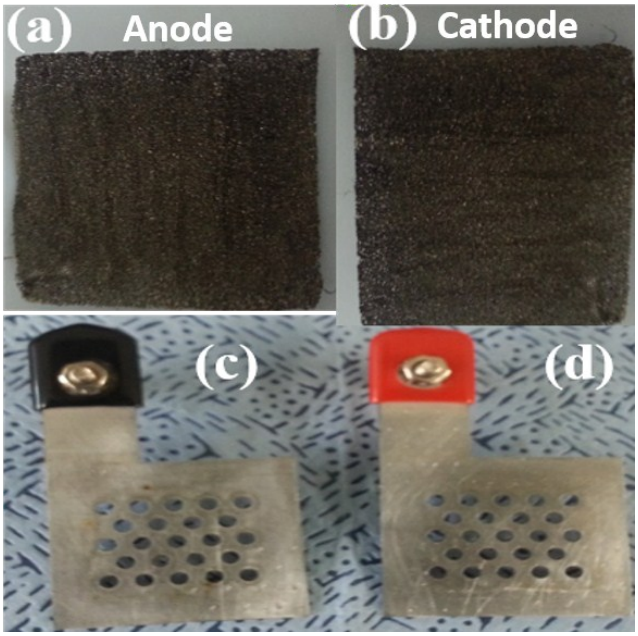

Fig. S2 (a) & (b) NiFeS-1/NF anode and cathode electrocatalysts of 1.5 cm^2 area. (c)& (d) Stainless steel electrodes used for alkaline electrolyte water electrolyzer.

7. Cyclic voltammetric

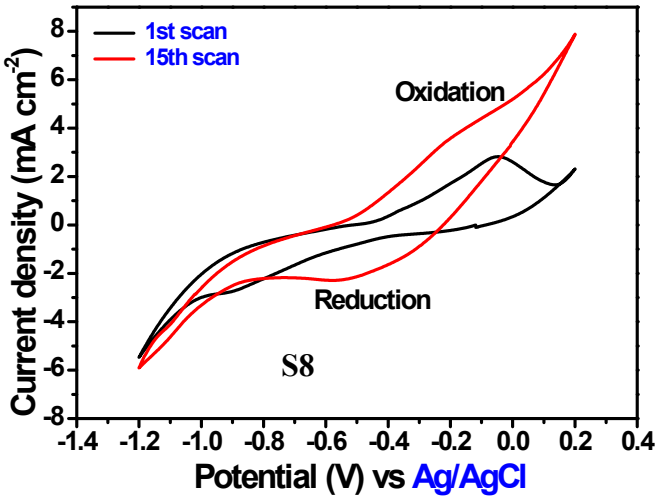

deposition step without thiourea on NiFe-1/NF and its corresponding XRD pattern.

(a)

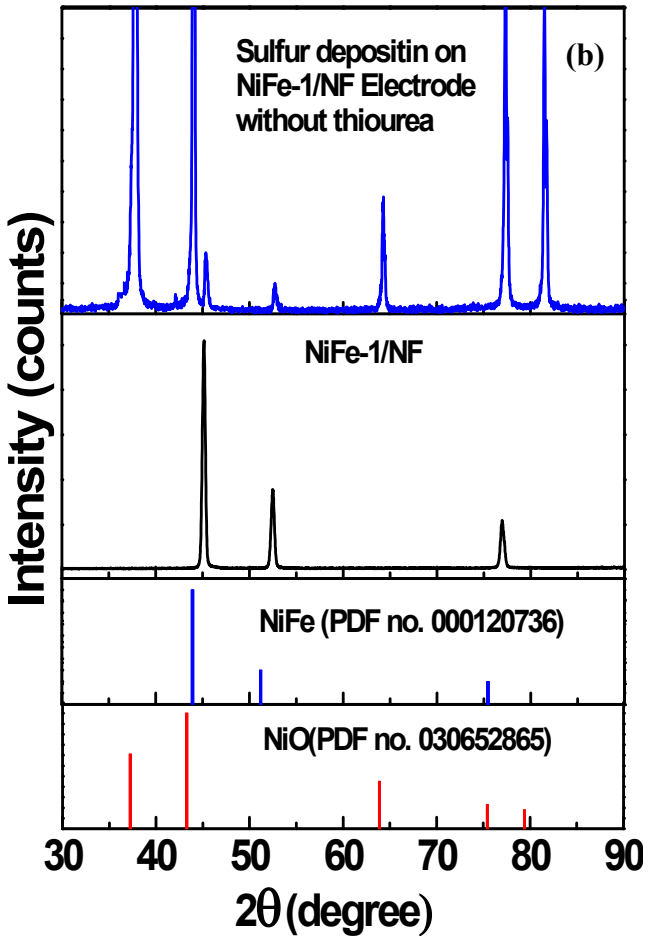

Fig. S3 (a) Cyclic voltammetry (CV) curve of the Nickel sulphide deposition on nickel foam.(b)XRD patterns of NiFe-1/NF and cyclic voltammetric deposition step without thiourea on NiFe-1/NF.

8. XRD pattern of Ni_3S_2/NF and NiFeS-1/NF after heat treatment

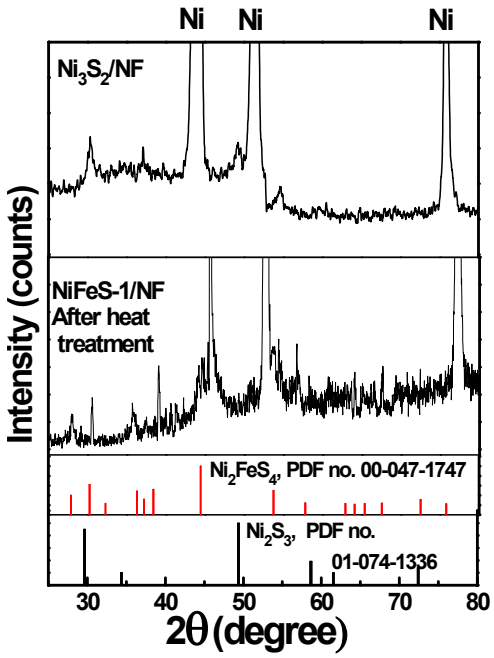

Fig. S4 XRD pattern of Ni_3S_2 deposited without iron deposition on NF and NiFeS-1/NF after heat treated to 500^0C in Argon atmosphere.

9. SEM morophology of NiFeS-2/NF

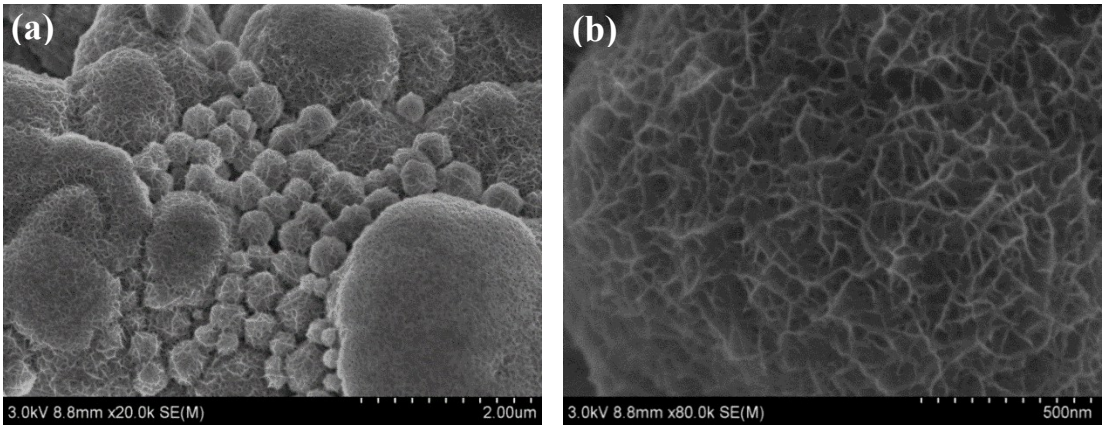

Fig.

S5

(a) Low and (b) high magnification SEM images of honey comb structured NiFeS-2/NF.

10. Energy dispersive X-ray analysis (SEM) on cross sectional NiFeS-1/NF

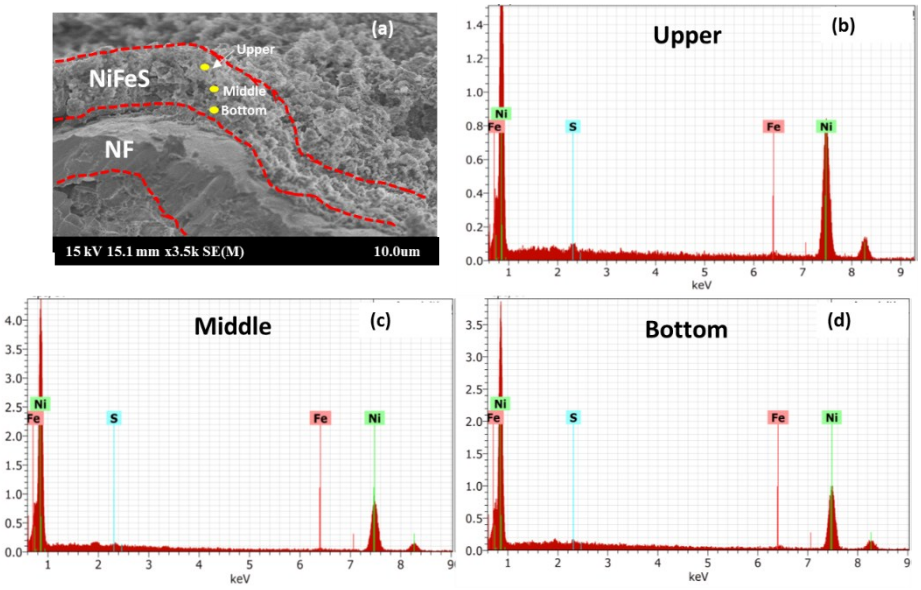

Fig. S6 (a) Cross sectional SEM images of NiFeS-1/NF with selected upper, middle and bottom regions (yellow points) of NiFeS coating on NF. (b) EDS elemental analysis of upper region, (c) EDS elemental analysis of middle region and (d) EDS elemental analysis of bottom.

11. TEM elemental mapping analysis of NiFeS-1/NF

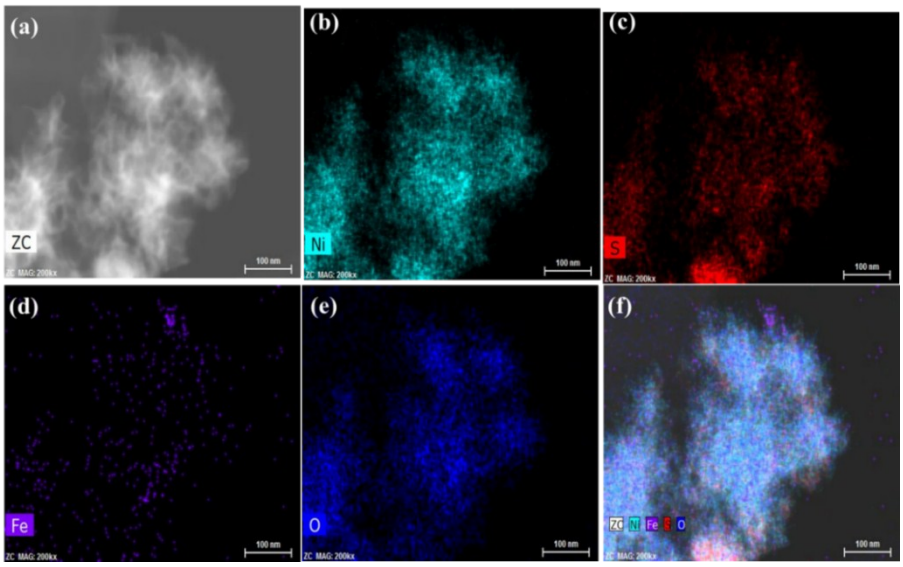

Fig. S7 (a) TEM elemental mapping analysis of NiFeS-1/NF (a) Selected area and corresponding elemental mapping for (b) Nickel, (c) Sulphur, (d) Iron, (e) Oxygen and (f) overlay image. Scale bar: 100 nm.

12. XPS spectra of NiFe-1/NF

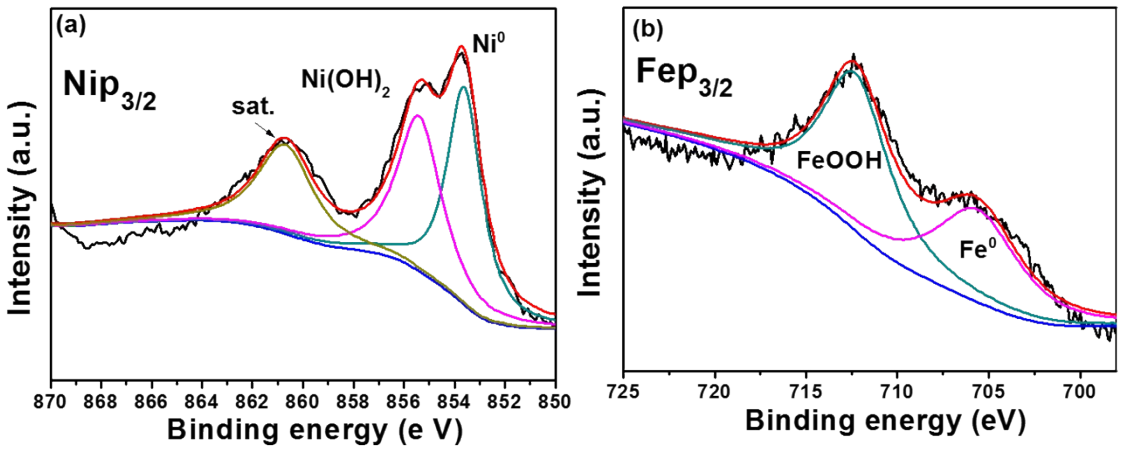

Fig. S8 (a) Nickel and (b) Iron XPS spectra of NiFe-1/NF.

13. OER and HER polarization of NiFeS-2/NF and NiFe-2/NF

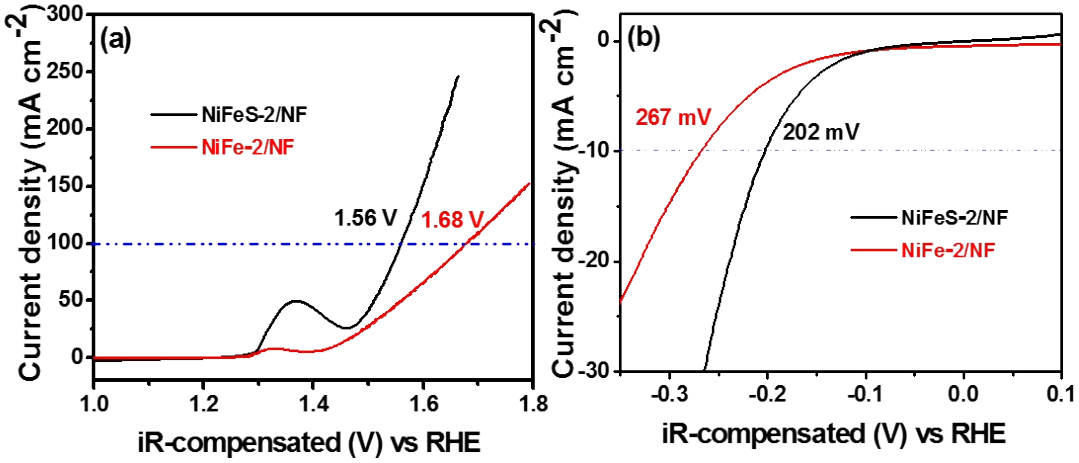

Fig. S9 (a) OER polarization traces of NiFeS-2/NF and NiFe-2/NF. (b) HER LSV polarization traces of NiFeS-2/NF and NiFe-2/NF in 1M KOH with a scan rate of 10 mV s^{-1}.

14. SEM morophology after durability

After 200h, OER test **After 200h, HER test**

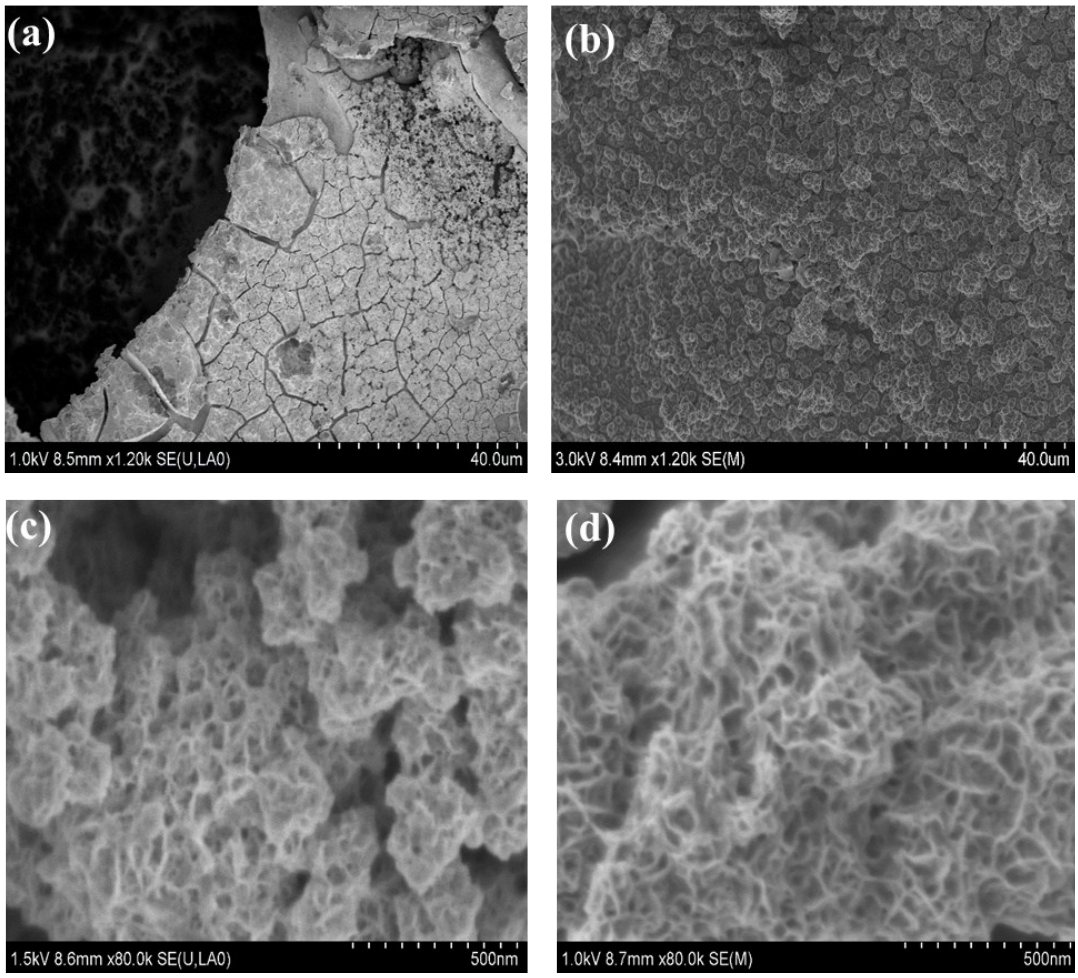

Fig. S10 (a) & (c) Low and high magnification images after 200 h OER durability. (b) Low & (d) high magnifications of NiFeS-1/NF electrode after 200 h HER durability.

15. XPS analysis after durability

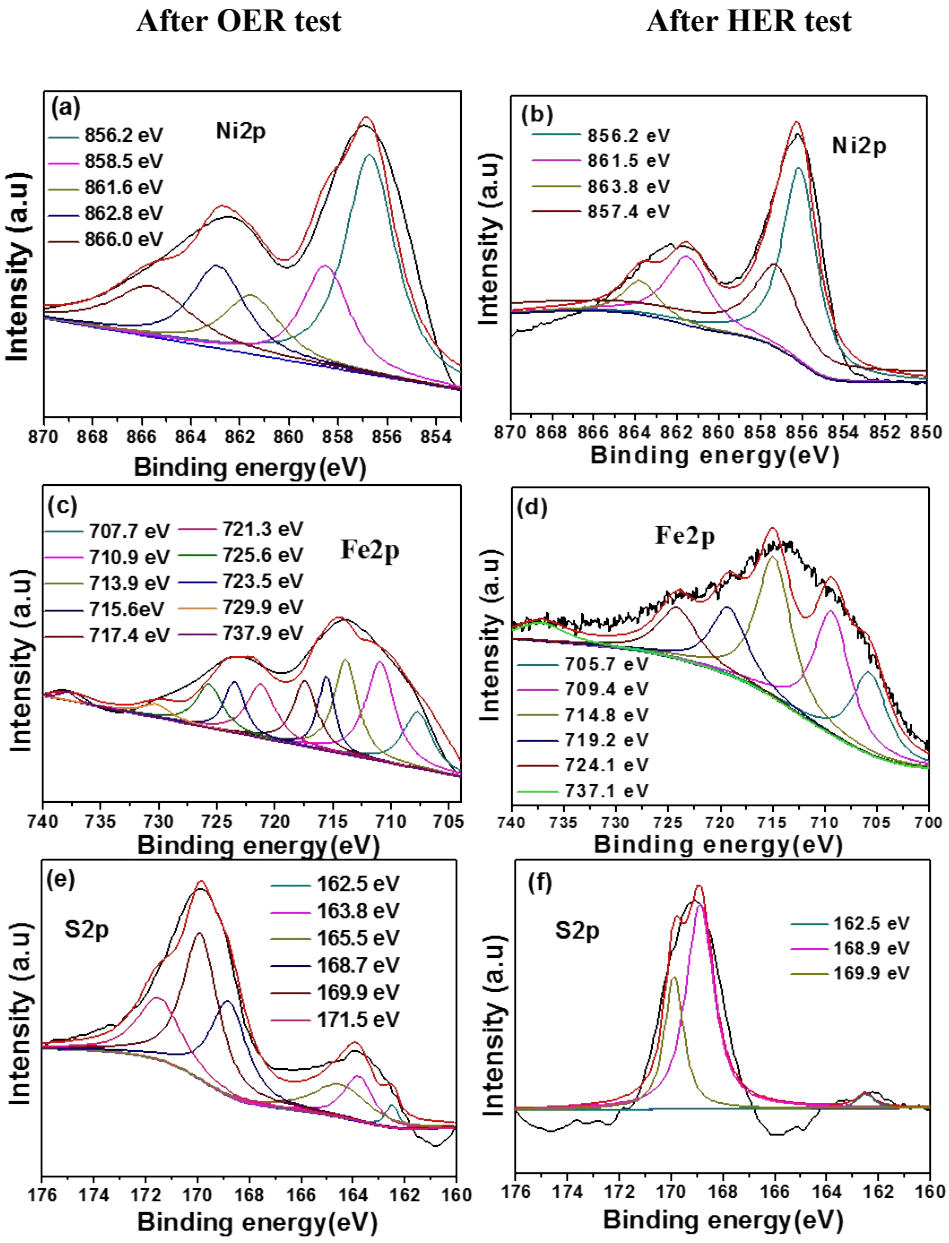

Fig. S11 (a) Nickel, (c) Iron and (e) Sulphur XPS spectra of the after OER durability of NiFeS-1/NF. (b) Nickel, (d) Iron and (f) Sulphur XPS spectra of the after HER durability of NiFeS-1/NF.

16. Comparitive XPS analysis of before and after durability tests

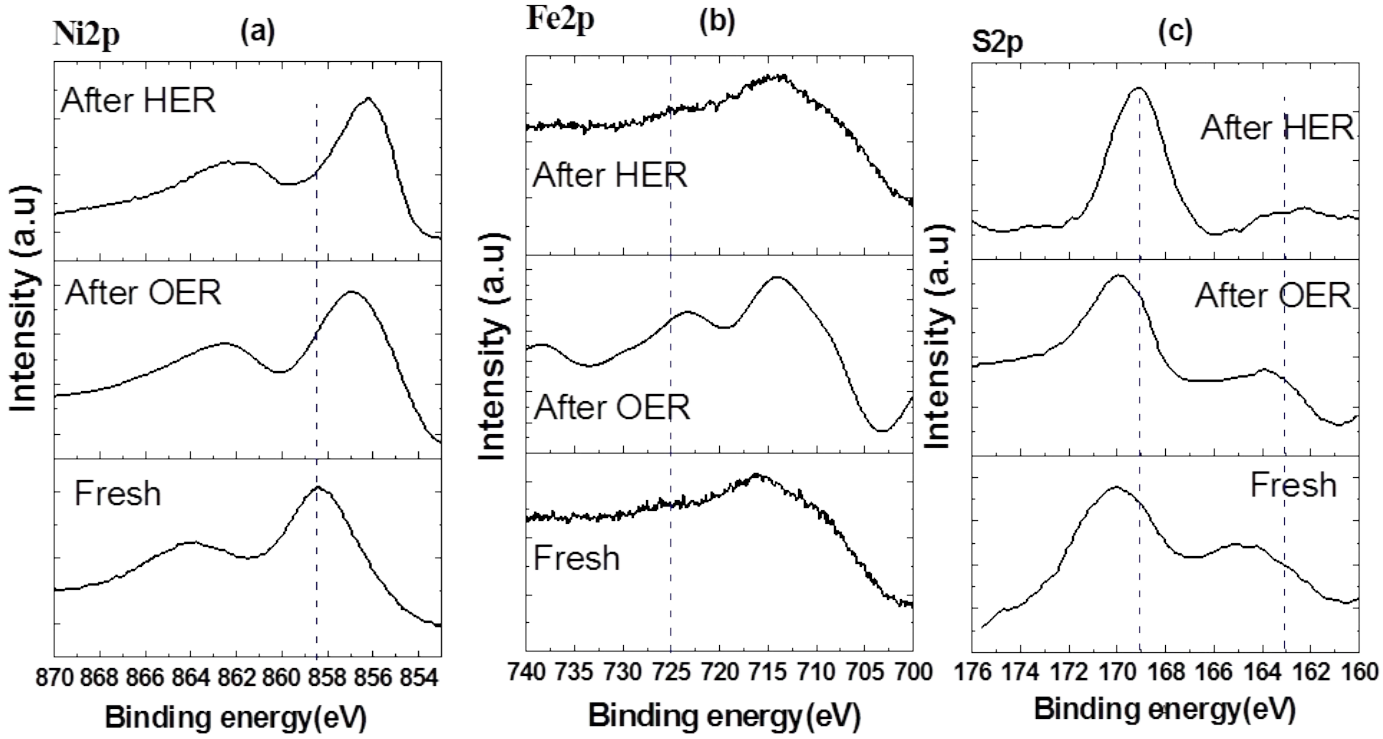

Fig. S12 (a) Nickel (Ni2p) XPS spectrum of fresh, after OER and HER durabilities, (b) Iron (Fe2p) XPS spectrum of fresh, after OER and HER durabilities and (c) Sulphur (S2p) XPS spectrum of fresh, after OER and HER durabilities.

17. Potentio-dynamic cyclic measurements of NiFeS-1/NF

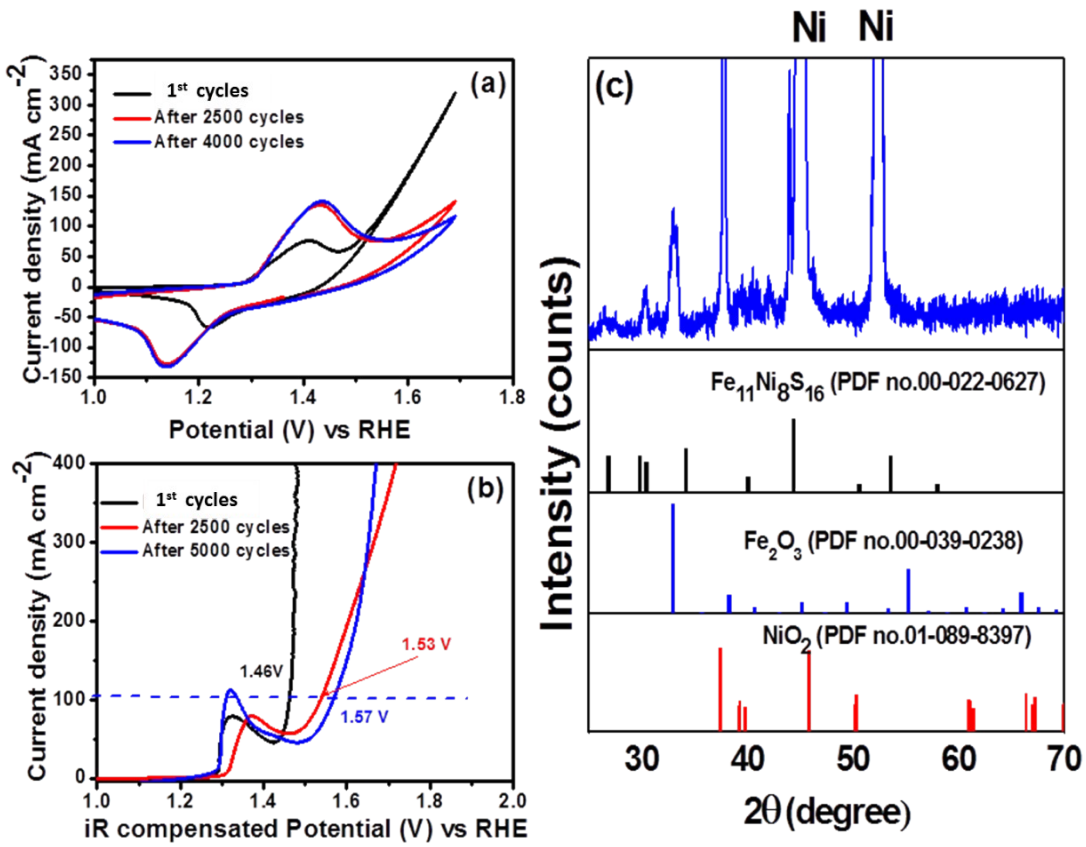

Fig. S13 (a) OER potentio-dynamic cyclability test for NiFeS-1/NF of fresh, after 2500 cycle and 5000 cycle. (b) OER durability test for NiFeS-1/NF fresh, after 3000 and after 5000 cycles. (c) XRD pattern of NiFeS-1/NF electorde after 5000 cycles of cyclic measurement.

18. SEM morophology after MEA performance

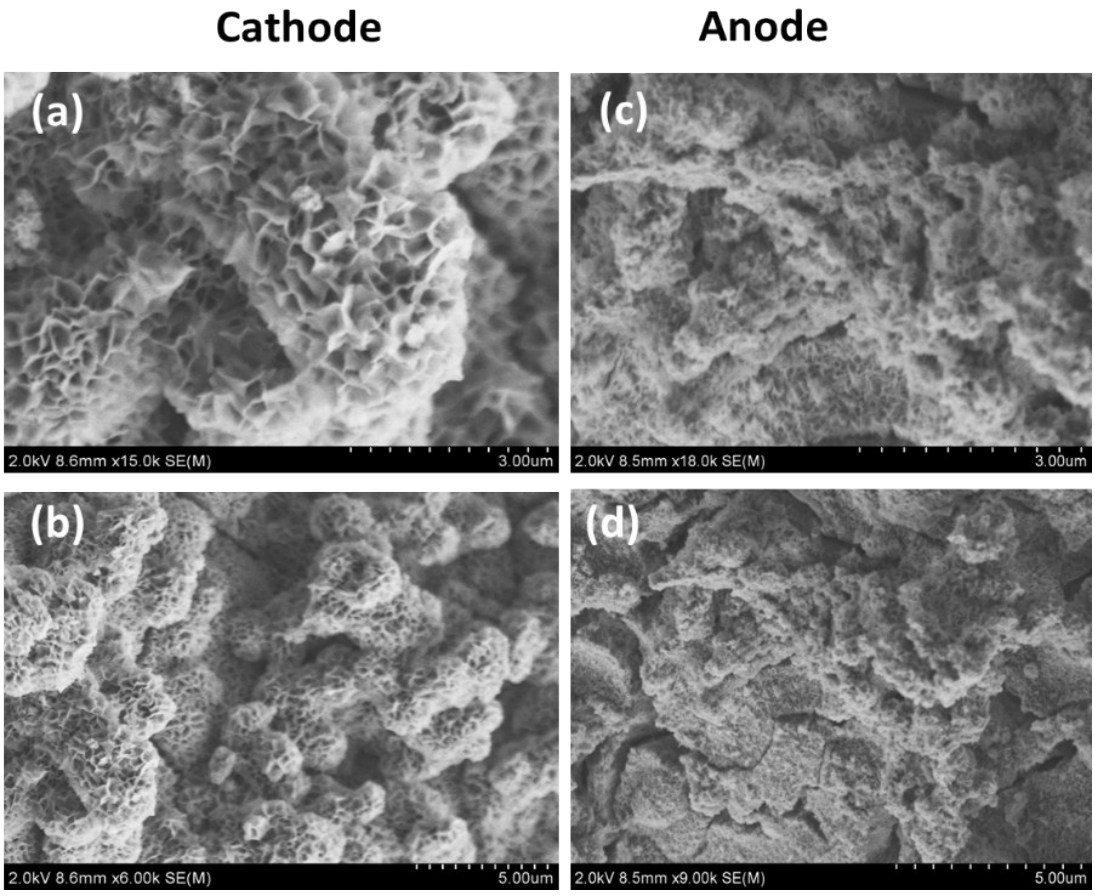

Fig. S14 (a)& (b) low and high magnification images of NiFeS-1/NF cathode after MEA performance. (c) Low & (d) high magnifications of NiFeS-1/NF anode after MEA performance.

EDS regions (inset in Figure S7)	Nickel Atomic (%)	Iron Atomic (%)	Sulfur Atomic (%)
Upper	**96.06**	**2.29**	**1.65**
Middle	**96.24**	**2.70**	**1.06**
Bottom	**96.60**	**2.44**	**1.10**

19. Table S1. Elemental compositions of EDX analysis from SEM in Cross section

20. References

1. M. Zahmakiran, T. Ayvali, S. Akbayrak, S. Caliskan, D. Celik, S. Ozkar, *Catalysis Today* 2011, **170**, 76-84.
2. D. S. Hall, D. J. Lockwood, C. Bock, B. R. MacDoughall, Proceedings A in Royal society publication, 2016, **A471**, 1-65.
3. A. P. Grosvenor, B. A. Kobe, M. C. Biesinger, N. S. Mclntyre, Surf. Interface Anal. 2004, **36**, 1564-1574.
4 H. Vrubel, X. Hu, *Angew. Chem., Int. Ed.* 2012, **51**, 12703–12706.
5 L. Marchetti, F. Miserque, S. Perrin, M. Pijolat, *Surf. Interface Anal.* 2015, **47**, 632–642.
6 M. Descostes, F. Mercier, N. Thromat, C. Beaucaire, M. Gautier-Soyer, *Appl. Surf. Sci.* 2000, **165**, 288–302.

7 A. R. Lennie, D. J. Vaughan, *Mineral Spectroscopy* 1996, **5**,117–131.

8 X. Liu, X. Qi, Z. Zhang, L. Ren, Y. Liu, L. Meng, K. Huang, J. Zhong, *Ceram. Int.* 2014, **40**, 8189–8193.

9 W. Zhu, X. Yue, W. Zhang, S. Yu, Y. Zhang, J. Wang, J. Wang, *Chem. Commun.* 2016, **52**,1486-1489.

10 X. Wu, B. Yang, Z. Li, L. Lei, X. Zhang, *RSC Adv.* 2015, **5**, 32976–32982.

11 W. Zhou, X. J.Wu, X. Cao, X. Huang, C. Tan, J. Tian, H. Liu, J. Wang, H. Zhang, *Energy Environ. Sci*. 2013, **6**, 2921-2924.

12 T. Yamashita, P. Hayes, *Appl. Surf. Sci.* 2008, **254**, 2441–2449.